DISCLAIMER

This report was prepared as an account of work sponsored by an agency of the United States Government. Neither the United States Government nor any agency thereof, nor any of their employees, makes any warranty, express or implied, or assumes any legal liability or responsibility for the accuracy, completeness, or usefulness of any information, apparatus, product, or process disclosed, or represents that its use would not infringe privately owned rights. Reference herein to any specific commercial product, process, or service by trade name, trademark, manufacturer, or otherwise does not necessarily constitute or imply its endorsement, recommendation, or favoring by the United States Government or any agency thereof. The views and opinions of authors expressed herein do not necessarily state or reflect those of the United States Government or any agency thereof. Reference herein to any social initiative (including but not limited to Diversity, Equity, and Inclusion (DEI); Community Benefits Plans (CBP); Justice 40; etc.) is made by the Author independent of any current requirement by the United States Government and does not constitute or imply endorsement, recommendation, or support by the United States Government or any agency thereof.

ORNL/TM-2025/3914

SCALE Analyses of Scenarios in the TRISO-Based Heat Pipe Microreactor Fuel Cycle

Donny Hartanto
Georgeta Radulescu
Friederike Bostelmann
William A. Wieselquist

June 2025

OAK RIDGE National Laboratory

ORNL IS MANAGED BY UT-BATTELLE LLC FOR THE US DEPARTMENT OF ENERGY

ORNL/TM-2025/3914

Nuclear Energy and Fuel Cycle Division

SCALE ANALYSES OF SCENARIOS IN THE TRISO-BASED HEAT PIPE MICROREACTOR FUEL CYCLE

Donny Hartanto
Georgeta Radulescu
Friederike Bostelmann
William A. Wieselquist

June 2025

Prepared by
OAK RIDGE NATIONAL LABORATORY
Oak Ridge, TN 37831
managed by
UT-BATTELLE LLC
for the
US DEPARTMENT OF ENERGY
under contract DE-AC05-00OR22725

CONTENTS

LIST OF FIGURES

LIST OF TABLES

LIST OF ABBREVIATIONS

CE	continuous energy
EFPY	effective full power year
HPMR	heat pipe microreactor
LWR	light-water reactor
MG	multigroup
non-LWR	non-light-water reactor
NRC	US Nuclear Regulatory Commission
PWR	pressurized water reactor
TRISO	TRistructural-ISOtropic

ACKNOWLEDGMENTS

This work was supported by the US Nuclear Regulatory Commission's Office of Nuclear Regulatory Research under Contract IAA 31310022S0011. The authors thank Cihangir Celik for the technical review of the report. The authors used ChatGPT (OpenAI, 2025) to assist in drafting and editing portions of the manuscript. All AI-assisted content was reviewed and edited by the authors to ensure accuracy and appropriateness.

ABSTRACT

This report documents the application of the SCALE code to the analysis of a TRistructural-ISOtropic (TRISO)-based heat pipe microreactor (HPMR) within the context of its nuclear fuel cycle stages. The evaluation was conducted in support of the US Nuclear Regulatory Commission's ongoing efforts to assess modeling capabilities for advanced non–light-water reactor technologies. The generic HPMR selected as a representative microreactor concept features a compact core design that incorporates TRISO fuel compacts, passive heat removal via heat pipes, and a transportable configuration intended for deployment in remote environments.

In this study, multiple SCALE analysis sequences were applied to evaluate representative hypothetical scenarios spanning the HPMR's operational and postoperational phases, including radionuclide inventory generation, criticality assessment, and radiation shielding analysis. Three bounding scenarios were defined. The focus of the first scenario was criticality scenarios during the transportation of the fresh core under both normal and accident conditions. The second scenario extended the analysis to the irradiated core, incorporating depletion modeling to generate postirradiation isotopic inventories and decay heat profiles with both static out-of-the-core and time-dependent control drum configurations. The third scenario addressed shielding calculations and dose rate evaluations during reactor operation and spent fuel transportation, including hypothetical accident conditions and unshielded dose assessments relevant to physical protection requirements.

Collectively, these scenarios demonstrate the applicability of the SCALE code system for performing integrated criticality, depletion, and shielding evaluations and safety assessments of compact, transportable microreactor designs.

1. INTRODUCTION

In recent years, advanced nuclear reactor technologies, especially non-light-water reactors (non-LWRs), have garnered considerable attention due to their potential for enhanced safety, operational efficiency, and versatility. To support the licensing and safe deployment of these emerging reactor designs, the US Nuclear Regulatory Commission (NRC) has prioritized evaluating computational codes employed in modeling accident progression, estimating radiological source terms, and conducting consequence analyses across operational and accident scenarios throughout the nuclear fuel cycle (US NRC 2020).

Central to these assessment activities are the SCALE (Wieselquist and Lefebvre 2023) and MELCOR (Humphries et al. 2021) code systems. Developed by Oak Ridge National Laboratory, the SCALE code system is used extensively for detailed neutronics analyses, including reactor physics assessments, radionuclide inventory characterization, criticality safety evaluations, and radiation shielding analyses. In parallel, the MELCOR code, developed by Sandia National Laboratories, is specifically tailored to simulate severe accident progression and perform evaluations of radioactive source terms. Together, these codes constitute an integrated modeling framework capable of capturing the entire progression of accident scenarios, from the determination of the initial state to potential release scenarios. Recent collaborative demonstrations have successfully showcased the combined capabilities of SCALE and MELCOR for various advanced reactor types, including heat pipe reactors (Walker et al. 2021; Wagner, Faucett, et al. 2022), high-temperature gas-cooled pebble-bed reactors (Wagner, Beeny, and Luxat 2022; Skutnik and Wieselquist 2021), fluoride salt cooled high-temperature reactors (Bostelmann et al. 2022; Wagner, Haskin, et al. 2022), molten salt fueled reactors (Lo et al. 2022; Wagner et al. 2023), and sodium-cooled fast reactors (Shaw et al. 2023; Wagner, Beeny, and Luxat 2023). Best practices and recommended methodologies for employing SCALE to model these specific reactor designs have been thoroughly documented in recent technical guidance (Bostelmann et al. 2024).

Building upon these foundational demonstrations, the NRC initiated a subsequent phase aimed at showcasing the comprehensive applicability of the SCALE and MELCOR code systems across the entirety of the nuclear fuel cycle for various non-LWRs (US NRC 2021). The initial steps of this effort involved the definition of representative nuclear fuel cycle stages for five distinct non-LWR technologies, along with a systematic identification of potential hazards and representative accident scenarios relevant at each fuel cycle stage (Bostelmann et al. 2023). Subsequently, illustrative accident scenarios were explicitly selected to highlight the capabilities and robustness of the computational codes independent of the probabilistic likelihood of these scenarios occurring.

As of now, three significant demonstrations using the SCALE code have been comprehensively documented: the first examining the scenarios in the fuel cycle of a high-temperature gas-cooled pebble-bed reactor (Elzohery et al. 2024), the second investigating a sodium-cooled fast reactor (Hartanto et al. 2024), and the third focusing on a molten salt reactor fuel cycle (Hartanto et al. 2025). This report documents the final demonstration in this series, focusing specifically on the scenarios in the nuclear fuel cycle associated with a TRistructural-ISOtropic (TRISO)-based heat pipe microreactor (HPMR). The generic HPMR design (Ortensi et al. 2024) was used as the initial model basis.

1.1 REFERENCE HEAT PIPE MICROREACTOR

The reference model for the HPMR employed in this analysis was derived from the generic monolithic HPMR design developed by Idaho National Laboratory (Ortensi et al. 2024). The fundamental dimensions and core configuration of the original design were retained, and several modifications were implemented to align the design with the specific objectives of this study. To ensure operation for a targeted lifespan of 3

effective full power year (EFPY) at a thermal power rating of 7.5 MW, the enrichment level of ^{235}U within the TRISO fuel kernels was increased from an initial 10.00 wt % in the original model to HALEU-level enrichments (i.e. 19.75 wt %). Additionally, the graphite reflector present in the initial design was replaced by a BeO reflector to enhance neutron economy.

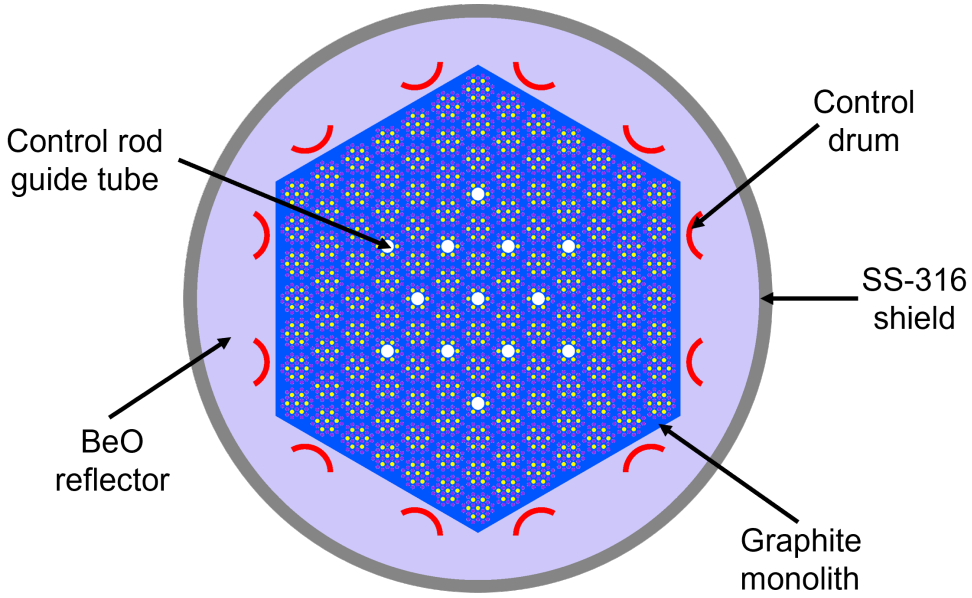

(a) Top view

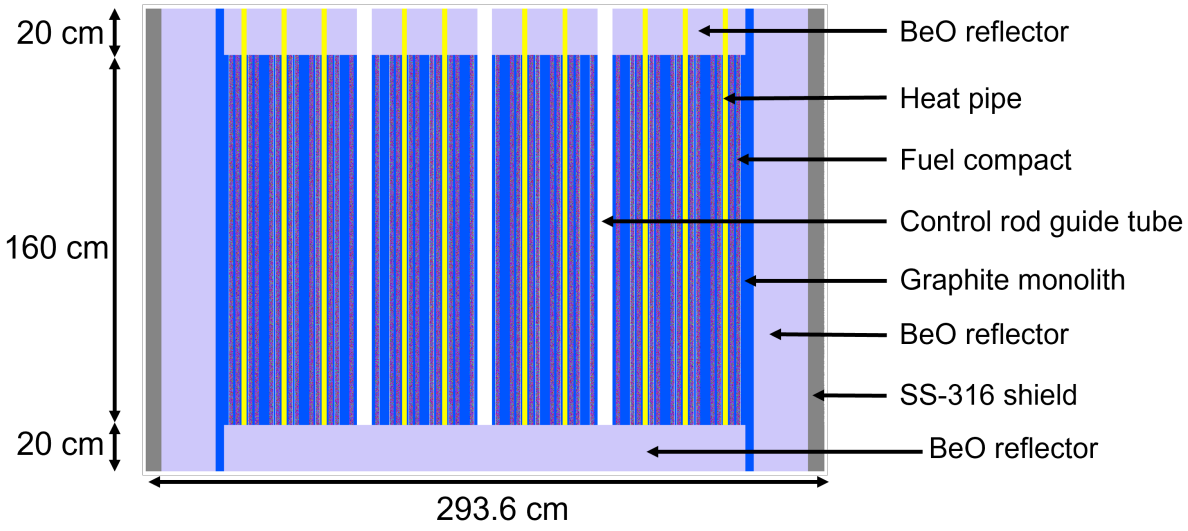

(b) Side view

Figure 1. SCALE HPMR model.

As illustrated in Figure 1, the reactor core is approximately 2 m in height and 3 m in diameter, and fuel assemblies are embedded within a graphite monolith. The axial ends of the core each incorporate a 20 cm thick BeO reflector. The bottom reflector is solid, whereas the top reflector incorporates channels to accommodate the heat pipes and control rods. The reactor core is enclosed by an outermost layer of stainless steel that functions simultaneously as a structural barrier and radiation shielding. Reactivity

control is managed by 13 shutdown control rods positioned within selected fuel assemblies and 12 control drums situated radially within the reflector region. Both control mechanisms employ B_4C absorbers containing naturally enriched ^{10}B. Table 1 summarizes the primary design parameters of the reference HPMR utilized in this study.

Table 1. Main design parameters of the reference HPMR

Parameter	Value
Reactor power	7.5 MWth
Core lifetime	3 EFPY
Kernel material	Uranium oxycarbide (UCO)
Kernel ^{235}U enrichment	19.75 wt %
Kernel density	10.5 g/cm^3
Kernel radius	0.02125 cm
Coating layer material	C/iPyC/SiC/oPyC
Coating layer thickness	100/40/35/40 μm
TRISO packing fraction	40%
Compact fuel zone radius	0.875 cm
Compact fuel zone height	2.45 cm
Compact nonfuel zone radius	0.90 cm
Compact nonfuel zone height	2.50 cm
Number of compacts per pin	64
Fuel assembly types	2
Number of standard fuel assemblies	114
Number of control rod fuel assemblies	13
Number of heat pipes	876
Fuel assembly pitch	17.368 cm
Pin pitch	2.782 cm
Reflector material	BeO
Monolith material	Graphite
Heat pipe coolant	Na
Number of control drums	12
Number of shutdown rods	13
Absorber material	B_4C

Two distinct types of fuel assemblies are utilized within the core, as shown in Figure 2. The first type, designated as the standard fuel assembly, contains 24 fuel pins. The second type, designated as the control rod fuel assembly, consists of 18 fuel pins arranged around a central hollow region designated for control rod insertion. Each fuel pin comprises an axial stack of 64 fuel compacts. Individual fuel compacts have a height of 2.50 cm (including fuel and nonfuel zones), cumulatively resulting in an active fuel height of approximately 160 cm per pin. The TRISO fuel particles and associated compacts utilized in this model are based on the AGR-2 specifications (Sowder and Marciulescu 2020). However, in this modified design, the packing fraction of TRISO particles in the compact is set at 40%, compared to the 37% in AGR-2 design.

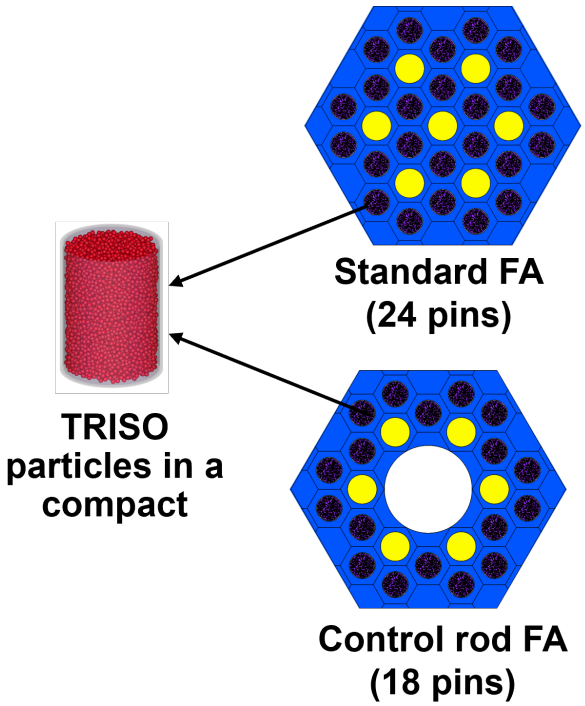

Figure 2. SCALE models of a fuel compact and the two fuel assembly types.

1.2 SELECTED ACCIDENT SCENARIOS

In this demonstration, three specific accident scenarios were selected from various stages of the HPMR nuclear fuel cycle. These scenarios were analyzed using the SCALE code system, and particular focus was given to criticality safety, radiation shielding, and radionuclide inventory. The following list summarizes the selected scenarios and associated analyses:

- **Criticality event during fresh fuel transportation:** The first scenario considers an accident during the transportation of fresh reactor fuel. In this scenario, a truck carrying the fresh HPMR core experiences an accident that results in the core package falling into a river and becoming submerged. Criticality analyses using SCALE were conducted to evaluate the reactor core's behavior under submerged conditions. Different cases were studied systematically, including scenarios in which water enters the core region and scenarios with or without displacement of the control rods.
- **Criticality event during spent fuel transportation:** The second scenario addresses the possibility of a criticality event during the transportation of spent (discharged) fuel. This scenario considers the changes in fuel characteristics after reactor operation. SCALE criticality analyses were performed for several potential accident conditions. As with the first scenario, different situations involving water ingress and changes in the arrangement of spent fuel were carefully examined.
- **Shielding analysis during the operation and transportation of spent fuel:** The third scenario evaluates radiation shielding effectiveness under two conditions: normal reactor operation and a transportation accident involving spent fuel. In the operational scenario, dose rates around the reactor enclosure were assessed to verify shielding adequacy. In the transportation scenario, the accident was assumed to compromise the integrity of the shielding surrounding the spent core. Radiation transport and dose rate analyses were performed using SCALE to evaluate shielding performance and to quantify potential radiation exposure under both nominal and postaccident conditions.

2. APPLIED SCALE SEQUENCES

SCALE is a comprehensive modeling and simulation suite for nuclear safety analysis and design (Wieselquist and Lefebvre 2023). The code includes verified and validated tools for criticality safety, reactor physics, radiation shielding, and radioactive source characterization. The work described in this report was primarily accomplished using three sequences of SCALE from version 6.3.2 and a development version of 7.0.

- **CSAS6-Shift:** SCALE's criticality safety analysis sequence (CSAS) (Goluoglu et al. 2011) can be used with SCALE's three Monte Carlo codes for the neutron transport calculations, e.g., KENO5, KENO6, Shift. CSAS can evaluate the criticality of complex 3D configurations under various conditions by calculating k_{eff}, the effective multiplication factor. This can cover, for example, analysis of fuel assemblies, reactor cores, or fuel storage configurations. In this work, CSAS was used with Shift, SCALE's new high-performance Monte Carlo code.
- **TRITON-Shift:** SCALE's TRITON sequence can be used for reactor physics and fuel depletion calculations (De Hart and Bowman 2011). TRITON couples SCALE's neutron transport solvers with the ORIGEN depletion solver to model the evolution of isotopes during reactor operation. TRITON can simulate both 2D and 3D reactor configurations, making it suitable for analyzing fuel assemblies and entire reactor cores. By calculating the fuel inventory as a function of time using the spectral conditions determined via the neutron transport calculations for the defined model (including the buildup of fission products, actinides, and other isotopes), TRITON generates a detailed radionuclide inventory. This inventory provides the basis for further analysis of spent fuel characteristics, decay heat, and more. This work applied TRITON in combination with the Shift Monte Carlo code to allow depletion of the 3D full HPMR core model.
- **MAVRIC-Shift:** SCALE's MAVRIC sequence is used primarily for radiation shielding and dose analysis. It performs fixed source radiation transport codes using Shift, along with an automated variance reduction method, to improve the efficiency and accuracy of radiation transport simulations, especially in complex geometries (Peplow 2011). MAVRIC uses an importance map generated by the Denovo deterministic code to guide particle tracking in Monte Carlo simulations, significantly reducing computational time while maintaining precision (Evans et al. 2010). Neutron and gamma source spectra determined using SCALE's depletion and decay modules can be accessed directly by MAVRIC, simplifying the input specifications. This work applies MAVRIC in combination with Shift. Given Shift's great performance for complex 3D problems, MAVRIC-Shift is an effective tool for shielding assessments of advanced reactor concepts, and it has been applied in recent studies for a variety of non-LWR systems (G. Radulescu and Wieselquist 2025).

All radiation transport calculations documented in this report were performed using the Shift Monte Carlo code (Pandya et al. 2016) in combination with a continuous energy (CE) or multigroup (MG) cross section library based on the ENDF/B-VII.1 nuclear data library (Chadwick et al. 2011). Shift in CE mode can model TRISO fuel compacts using the enhanced geometry handling capabilities introduced in SCALE 6.3.2. Two methods for TRISO particle placement are available: (1) the random method, which stochastically populates a specified volume with nonoverlapping particles to achieve a target packing fraction (e.g., 40% or higher), and (2) the replica method, which creates an explicit particle distribution within a reference block and replicates it across the geometry (Ghaddar et al. 2024). On the other hand, Shift in MG mode supports the SCALE double-heterogeneity treatment for TRISO fuel using group-structured cross sections and embedded double-heterogeneity treatment (Bostelmann et al. 2020; Kim et al. 2021), which provides computational efficiency for extensive calculations (e.g., depletion).

3. SCENARIO 1: CRITICALITY EVENT DURING FRESH FUEL TRANSPORTATION

The transportation of a fresh HPMR core introduces a unique criticality safety challenge. The monolithic core has high initial reactivity due to the enriched fresh fuel, which makes water immersion scenarios particularly important from a safety perspective. Although the probability of a severe accident resulting in core immersion is very low, road transportation inevitably involves crossing bridges or routes near bodies of water, meaning that such immersion scenarios are credible accident conditions. Accordingly, 10 CFR 71 regulations explicitly require evaluating the criticality safety of transportation packages under water immersion accidents (Code of Federal Regulations Title 10 Part 71). Water significantly enhances neutron moderation and reflection, which can substantially increase the core's k_{eff}. Therefore, a scenario in which a vehicle transporting a fresh reactor core plunges into a river or lake was analyzed, as required by 10 CFR 71, to assess whether the core design can reliably maintain subcritical conditions ($k_{\text{eff}} \leq 0.95$) under such an accident scenario and to evaluate the performance of SCALE in this context.

For this scenario, a SCALE/CSAS6-Shift model was developed. The fresh core was placed at the center of a large water body with a 100 cm thick water layer extending in all directions, as presented in Figure 3. Although preliminary sensitivity analyses showed that peak reactivity occurs with approximately 10 cm of water thickness (as shown in Figure 4 for the full immersion case with control drums and control rods inserted), the thicker layer of 100 cm was selected to conservatively simulate immersion in an unrestricted large body of water. The observed slight decrease in reactivity beyond 10 cm can be attributed to the transition from optimal moderation to an over-moderated condition, in which further increases in water thickness increase neutron capture by the water.

The model explicitly includes control rods and control drums (both containing natural boron carbide absorbers), and all components are at room temperature. Two distinct water ingress conditions were considered in the analysis. The first condition, referred to as partial immersion, assumes that water surrounds only the exterior of the core without penetrating internal void spaces, such as fuel compact gaps or control rod guide tubes. The second condition, full immersion, represents complete water ingress into all internal and external core void spaces. Additionally, criticality calculations were conducted for various control rod positions (fully inserted or fully withdrawn) and control drum orientations (absorber facing inward or outward). The eight configurations analyzed are summarized in Table 2. Each simulation used 100,000 neutron histories per cycle, with 100 inactive cycles. The number of active cycles was determined automatically to ensure that the statistical uncertainty in the k_{eff} remained below 10 pcm.

Table 2. Simulated cases for the fresh HPMR core

Case	Water ingress	Control rod position	Control drum orientation
A-1	Partial	Out	Outward
A-2	Partial	Out	Inward
A-3	Partial	In	Outward
A-4	Partial	In	Inward
B-1	Full	Out	Outward
B-2	Full	Out	Inward
B-3	Full	In	Outward
B-4	Full	In	Inward

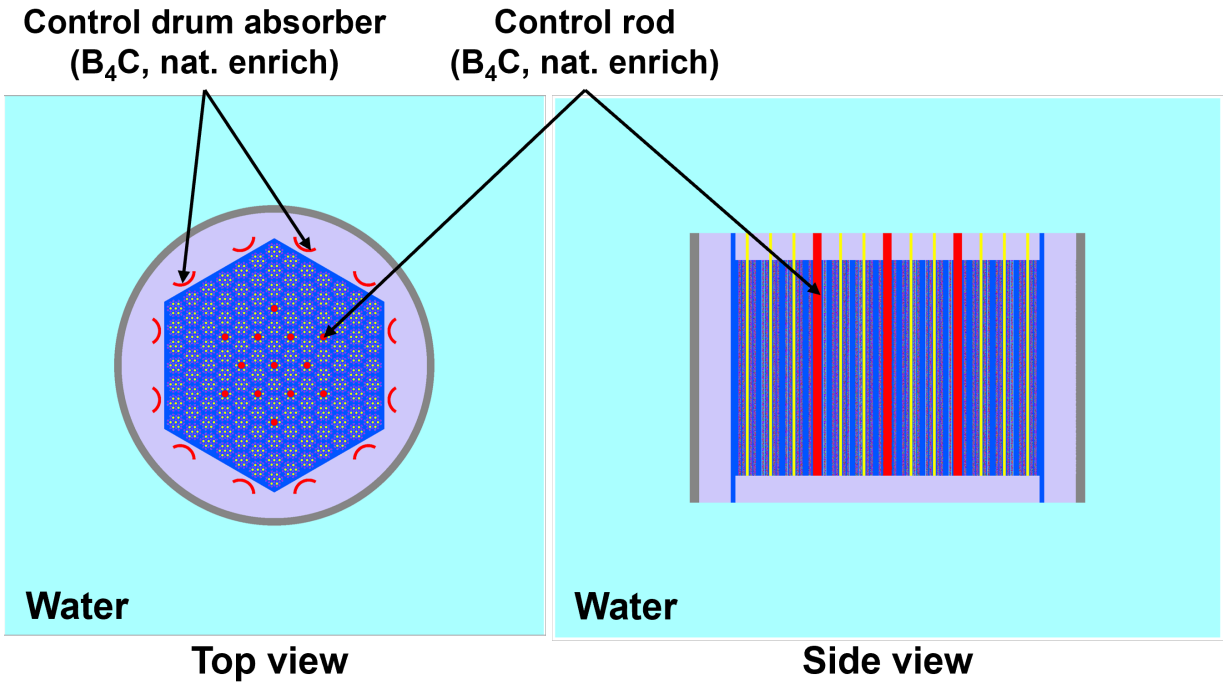

Figure 3. Criticality model of HPMR core immersed in water.

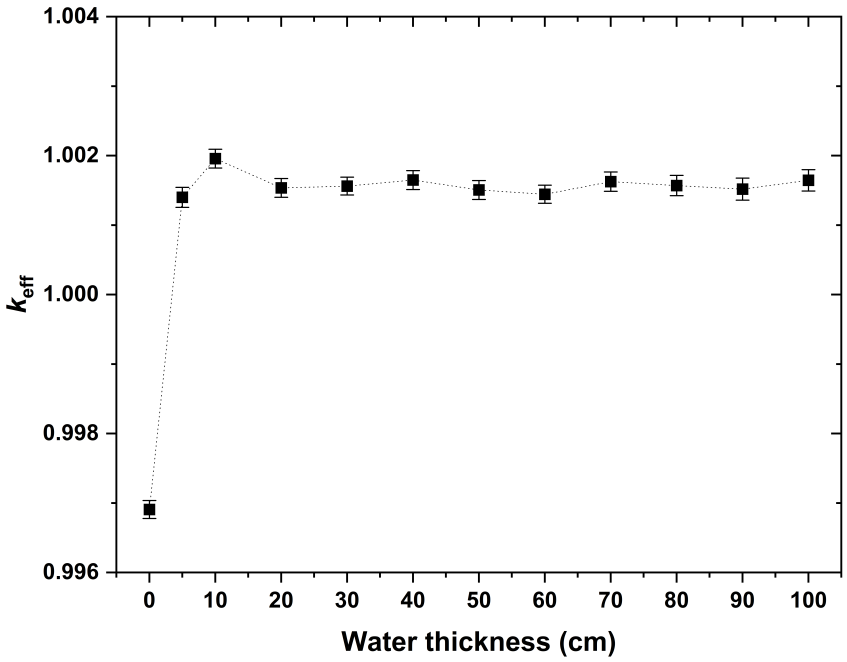

Figure 4. Multiplication factor as a function of surrounding water thickness for full immersion case with control drums and control rods inserted. Error bars indicate 1σ (one standard deviation) statistical uncertainties.

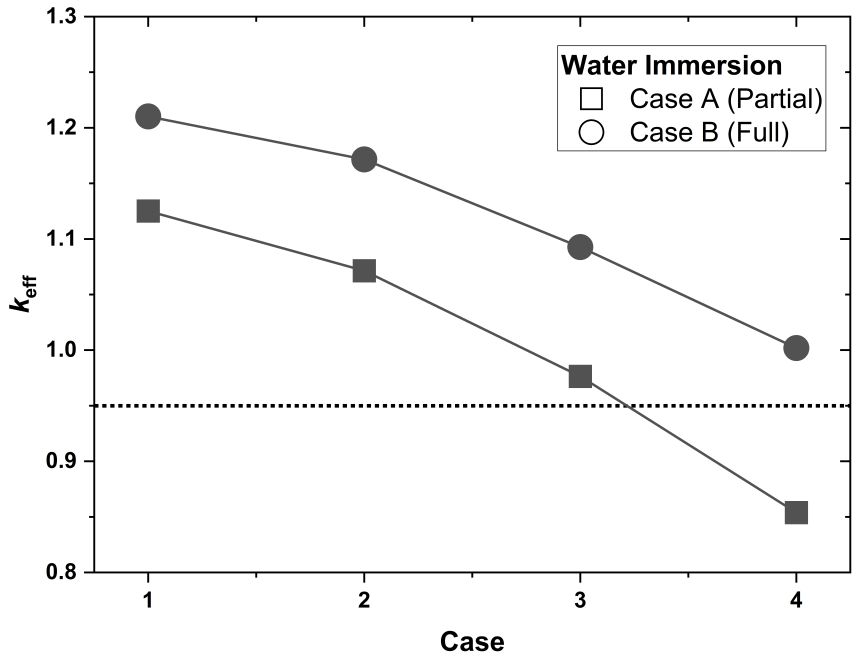

Figure 5. Multiplication factor of the submerged fresh HPMR core in various configurations corresponding to Table 2.

The results, presented in Figure 5, indicate that among the partial immersion scenarios, only Case A-4, in which control rods are fully inserted and drum absorbers face inward, satisfies the regulatory limit of 0.95, resulting in a calculated k_{eff} of 0.85392 ± 0.00013. Under full immersion conditions, however, reactivity increases substantially. The most reactive configuration (Case B-1, control rods withdrawn and drum absorbers outward) yields a k_{eff} of 1.210285 ± 0.00014, which far exceeds the regulatory limit. Even in the best control scenario for full immersion (Case B-4), the core remains supercritical with a k_{eff} of 1.001851 ± 0.00015, which corresponds to an additional negative reactivity requirement of approximately 5,185 pcm. This increase in reactivity is primarily attributable to enhanced neutron thermalization from water ingress, as evidenced by the neutron energy spectrum (Figure 6) showing a significant increase in thermal neutron flux below 1 eV.

To explore potential methods for improving criticality safety margins, further sensitivity studies were performed by increasing the ^{10}B enrichment in the B_4C absorbers to 90%, 95%, and 99%. These enriched absorbers provided an additional negative reactivity of approximately 2,000 pcm, as shown in Figure 7. However, this was still insufficient to achieve subcritical conditions for the fully immersed core. Therefore, additional or alternative criticality control measures would be necessary to transport the HPMR core in the configuration that is studied in this work. Possible strategies include introducing additional absorber rods, incorporating burnable neutron absorbers within the core structure, and employing engineered barriers designed specifically to prevent internal water ingress.

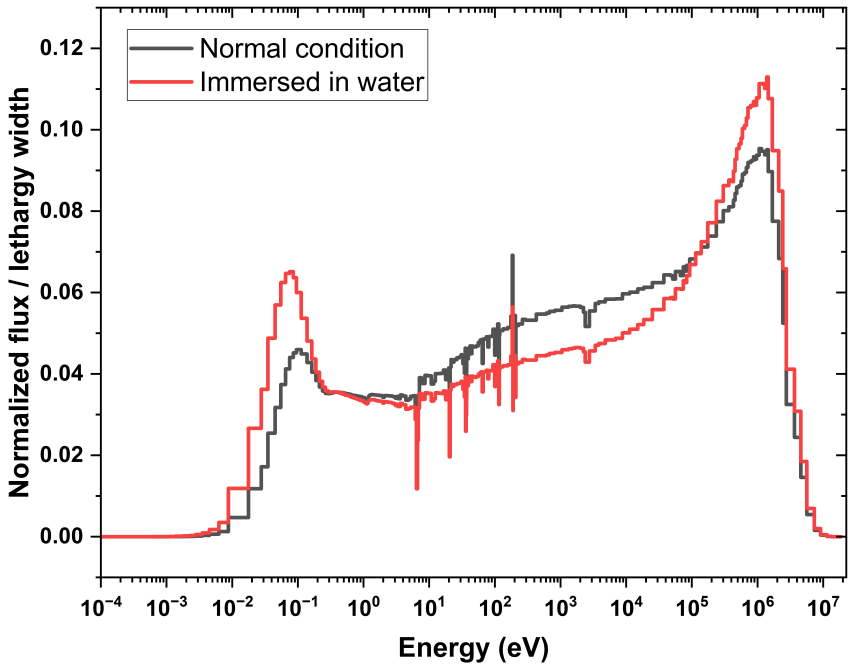

Figure 6. Comparison of neutron spectra in kernel at normal condition and when immersed in water.

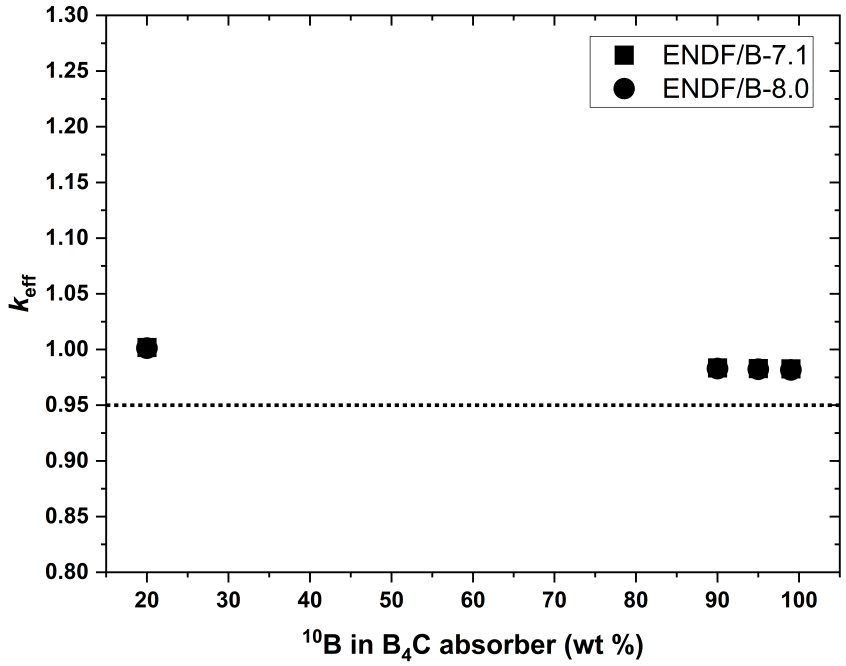

Figure 7. Multiplication factor of the fresh HPMR core at full immersion with fully inserted control drums and control rods at different ^{10}B enrichment levels.

4. SCENARIO 2: CRITICALITY EVENT DURING IRRADIATED FUEL TRANSPORTATION

In comparison with the transportation of fresh nuclear fuel, the transportation of irradiated nuclear fuel has distinct criticality and radiological safety considerations due to isotopic changes resulting from irradiation, including the buildup of fission products and transuranic isotopes. Accurate modeling of fuel depletion and the resulting spent fuel isotopic inventory is therefore a first step in evaluating criticality and radiation source terms during the transportation of irradiated cores. Consequently, detailed depletion calculations were performed to generate a realistic isotopic inventory necessary for subsequent criticality analyses since fission products have a significant effect on reactivity;.

4.1 DEPLETION CALCULATION

The depletion analyses for the HPMR core were conducted using SCALE/TRITON-Shift, as described in Section 2. Shift was run in MG mode to take advantage of the computational efficiency and established accuracy of the MG approach when simulating double-heterogeneous fuel configurations, such as those involving TRISO fuel particles embedded within graphite matrices like in HPMR core (Bostelmann et al. 2020; Kim et al. 2021). To verify the accuracy and reliability of the MG approach for this application, a comparative analysis was performed using the development version of SCALE 7.0 against CE Monte Carlo calculations. The TRISO particles embedded in fuel compacts were modeled using the random packing option, as discussed in Section 2. The results of this comparison, summarized in Table 3, demonstrate excellent agreement between the MG and CE calculations, with discrepancies in k_{eff} below 80 pcm. Additionally, the MG calculations achieved a computational speed approximately 7× faster than that of comparable CE calculations, confirming the suitability and practicality of the MG methodology for computationally intensive depletion analyses.

Table 3. Comparison between CE and MG of k_{eff} of HPMR 3D core

Case	Library	k_{eff}	Difference (pcm)	Speed-up factor
Control drum facing core	CE	0.99897 ± 0.00031	-	-
	MG-252g	0.99972 ± 0.00022	75.6 ± 38.0	6.65
Control drum facing outwards	CE	1.05522 ± 0.00026	-	-
	MG-252g	1.05594 ± 0.00017	72.3 ± 31.1	7.69

To assess the sensitivity of the irradiated fuel inventory and resulting decay heat characteristics, two distinct depletion scenarios were considered. In the first scenario, all control rods and control drum absorbers were assumed to remain fully withdrawn (i.e. faced outwards) throughout the entire irradiation cycle. In the second scenario, a dynamic control strategy was adopted in which the angular positions of control drum absorbers were periodically adjusted during depletion to maintain the core near critical conditions over its operational lifetime. To facilitate this dynamic depletion scenario, a Python-based script was developed to interface directly with SCALE/TRITON-Shift. At the beginning of each 30 day depletion interval, eigenvalue calculations were performed using SCALE/CSAS6-Shift for a series of control drum angles. These eigenvalues were subsequently fitted using a sixth-order polynomial to model reactivity as a function of control drum position. An illustration of the control drum worth curve calculated at fresh core is provided in Figure 8. Brent's root-finding method was then applied to identify the optimal drum angles required to achieve an initial excess reactivity of approximately 400 pcm at the beginning of each depletion step to ensure that the reactor remained close to critical throughout its operation. With these updated

control drum positions determined, the SCALE/TRITON-Shift depletion calculation proceeded accordingly until the target lifetime. Additionally, recent modeling enhancements introduced in the SCALE version 7.0 beta were utilized. Notably, these enhancements enabled depletion calculations directly based on total reactor thermal power (MWth) rather than the traditional method of specific power (MWth per initial tonne of heavy metal) and avoided conventional heavy metal mass normalization in the output and binary inventory file (file f71).

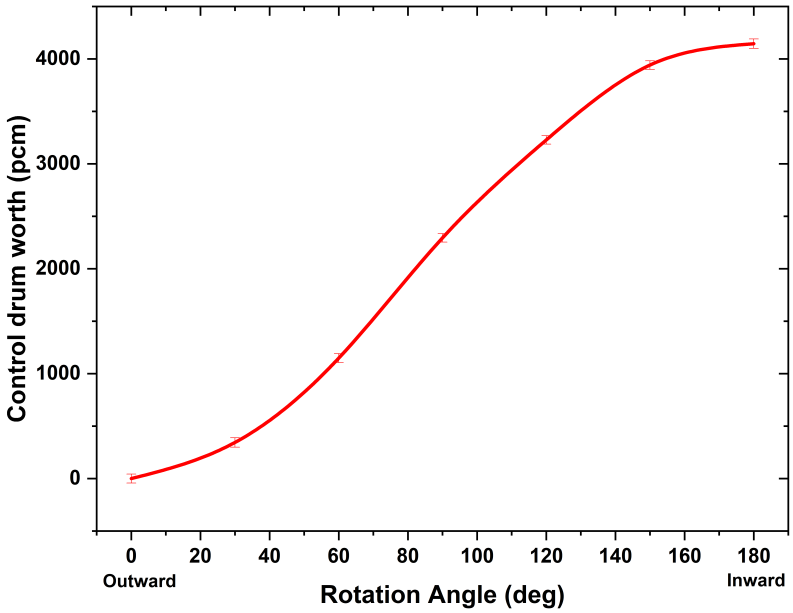

Figure 8. Control drum worth as function of the absorber orientation.

Figure 9 shows the calculated evolution of k_{eff} throughout the operating lifetime for both depletion cases, along with the corresponding angular positions of the control drums required to manage the excess reactivity over time. These results clearly illustrate the capability of the control drum positioning to maintain near-critical conditions throughout core life. Following the completion of these depletion simulations, detailed analyses of the isotopic compositions within the irradiated fuel were conducted. To contextualize these results, a comparison was made against the spent fuel composition from a representative pressurized water reactor (PWR) with an initial ^{235}U enrichment of 4.2 % and a discharge burnup of 50 GWd/tU. As anticipated, the lower burnup of the HPMR core (approximately 15.88 GWd/tU after 3 EFPY) resulted in a significantly lower mass fraction of fission products (approximately 1.48%) in comparison with approximately 4.55% in the discharged PWR fuel, as shown in Figure 10. Both HPMR depletion scenarios showed similar isotopic distributions. However, the scenario employing dynamic control drum positioning exhibited a modest neutron spectral hardening, as reflected by an approximate 3% increase in ^{239}Pu content relative to the conventional scenario in which control rods and drums remained fully withdrawn.

Figure 11 shows a comparison of the decay heat of the discharged fuel from the HPMR and a PWR. Immediately following reactor shutdown, decay heat amounted to approximately 6% of the operating power. This value is consistent with typical values observed in PWRs. Additionally, the decay heat profiles of both HPMR depletion cases showed a similar trend. Due to the relatively lower burnup achieved by the HPMR, dominant contributors to decay heat differed notably from the PWR case, as summarized in Table 4. Actinides such as ^{239}U and ^{239}Np, which are significant decay heat contributors in high-burnup

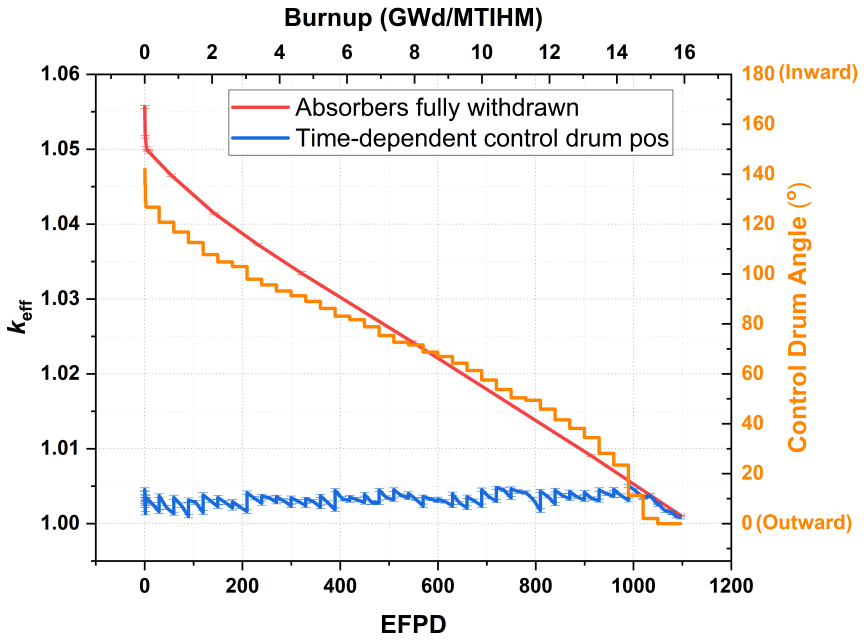

Figure 9. Evolution of k_{eff} as function of days with and without time-dependent control drums' position.

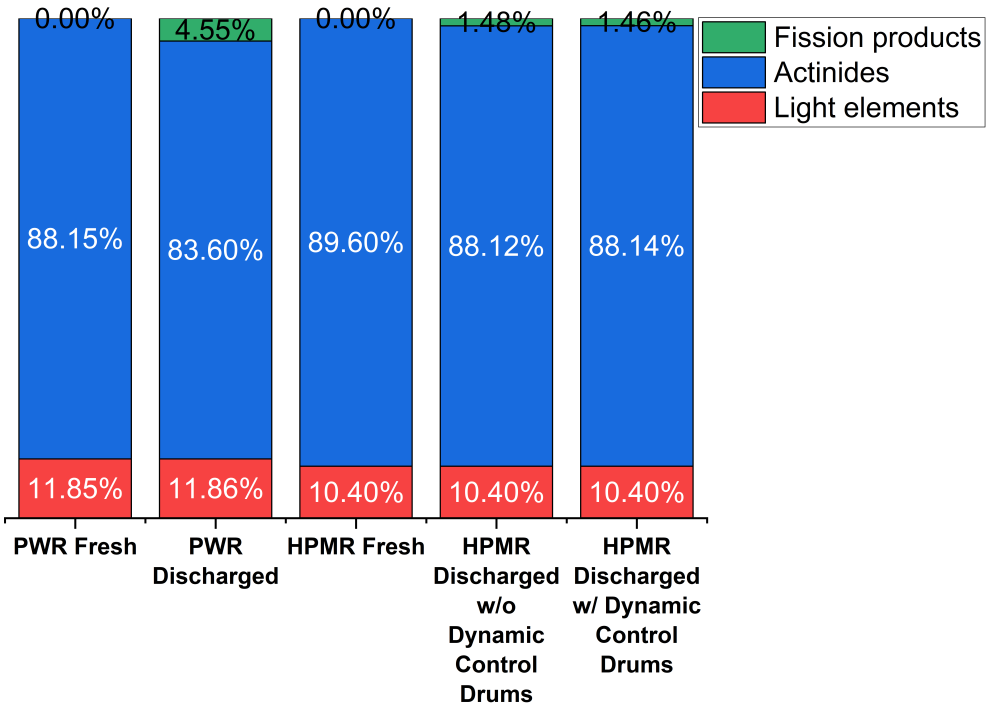

Figure 10. Comparison of composition distribution in spent fuel between the HPMR and a PWR.

PWR spent fuel, were absent from the top five contributors to the initial decay heat in the HPMR. Short-lived fission products were predominant instead.

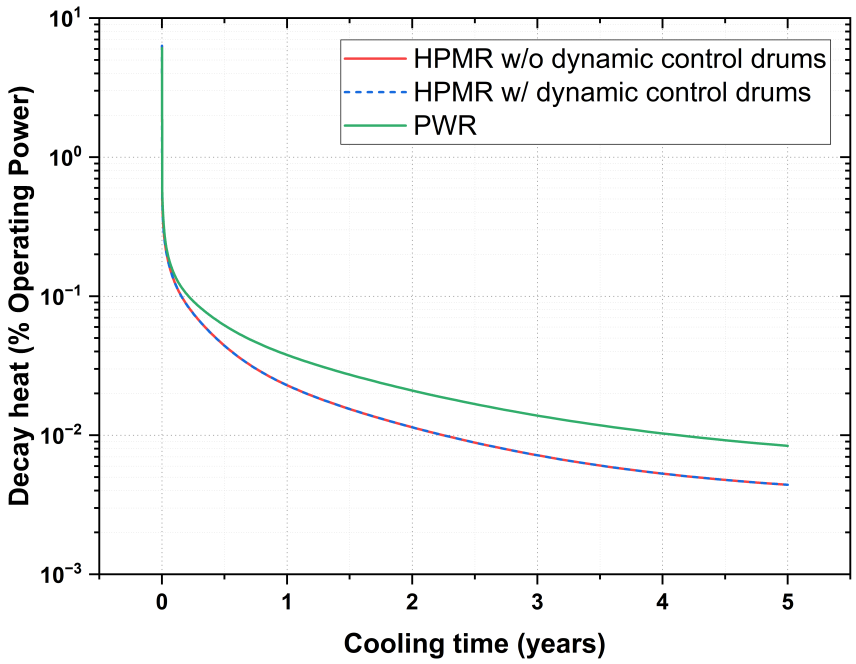

Figure 11. Comparison of decay heat between HPMR and PWR.

Table 4. Top five contributors of decay heat in the HPMR and PWR

Shutdown		After 5 years of cooling	
HPMR	PWR	HPMR	PWR
^{134}I (1.94%)	^{239}U (2.73%)	^{90}Y (36.09%)	^{134}Cs (18.78%)
^{138}Cs (1.87%)	^{239}Np (2.39%)	^{137m}Ba (26.05%)	^{90}Y (18.54%)
^{92}Rb (1.77%)	^{134}I (1.89%)	^{144}Pr (8.17%)	^{137m}Ba (18.38%)
^{144}La (1.72%)	^{138}Cs (1.76%)	^{90}Sr (7.57%)	^{244}Cm (8.37%)
^{91}Rb (1.66%)	^{104}Tc (1.64%)	^{137}Cs (7.46%)	^{106}Rh (7.80%)

4.2 CRITICALITY ANALYSIS

The criticality of the irradiated HPMR core during transportation was evaluated under hypothetical water immersion conditions resulting from a severe vehicle accident, consistent with the analyses performed for the fresh core. The SCALE/CSAS6-Shift model previously employed for the fresh core analysis was applied again here. To accurately represent the irradiated fuel condition, isotopic compositions corresponding to three cooling intervals—immediately after discharge, 1 year after discharge, and 5 years after discharge—were derived from the depletion calculations presented in the previous section. Following regulatory guidance from NUREG-2216 (Borowski et al. 2020), these compositions included only key nuclides recommended for burnup credit analyses: specifically, major actinides and select fission products, along with carbon and oxygen as intrinsic components of the uranium oxycarbide fuel kernel. The specific nuclides included are summarized in Table 5. It should be noted that this set of nuclides was originally

developed for light-water reactors (LWRs), and their application here is intended for illustrative purposes only.

Table 5. Nuclide sets considered for criticality analysis of spent HPMR fuel (Borowski et al. 2020)

Type	Nuclide Set
Actinide only	^{234}U, ^{235}U, ^{238}U, ^{238}Pu, ^{239}Pu, ^{240}Pu, ^{241}Pu, ^{242}Pu, ^{241}Am
Actinide plus fission products	^{95}Mo, ^{99}Tc, ^{101}Ru, ^{103}Rh, ^{109}Ag, ^{133}Cs, ^{143}Nd, ^{145}Nd, ^{147}Sm, ^{149}Sm, ^{150}Sm, ^{151}Sm, ^{152}Sm, ^{151}Eu, ^{153}Eu, ^{155}Gd, ^{236}U, ^{237}Np, ^{243}Am

Similar to the analyses conducted for the fresh core transportation scenario, criticality calculations were performed for multiple irradiated core configurations. These calculations included scenarios involving partial and full water immersion combined with different control rod states (fully inserted or withdrawn) and control drum orientations (absorbers inward or outward). Figure 12 shows the calculated k_{eff} for the irradiated core under both immersion conditions and at various cooling times. Two primary observations emerged from these results. First, under partial immersion conditions, inserting the control rods alone is sufficient to achieve the regulatory subcriticality limit of $k_{\text{eff}} \leq 0.95$, even without engaging control drums, as demonstrated by Case A-3. This behavior is anticipated because irradiation reduces fissile material inventory and leads to the buildup of neutron-absorbing fission products, significantly lowering the core's excess reactivity. Second, despite the reduced reactivity relative to the fresh core, the full immersion scenarios, exemplified by Case B-4, still exceed the criticality safety threshold. Even in the optimal configuration, in which control rods are fully inserted and drum absorbers are facing inward, the system remains slightly supercritical, indicating that additional negative reactivity measures would be necessary to achieve compliance under these conditions. Furthermore, the effect of cooling time was evaluated, revealing minimal differences in k_{eff} of less than 150 pcm between the 1 year and 5 year cooling cases. This limited discrepancy is expected when employing the selected nuclide sets because the decay of the short-lived fission products only slightly reduces reactivity, whereas long-lived actinides remain relatively constant over these cooling intervals.

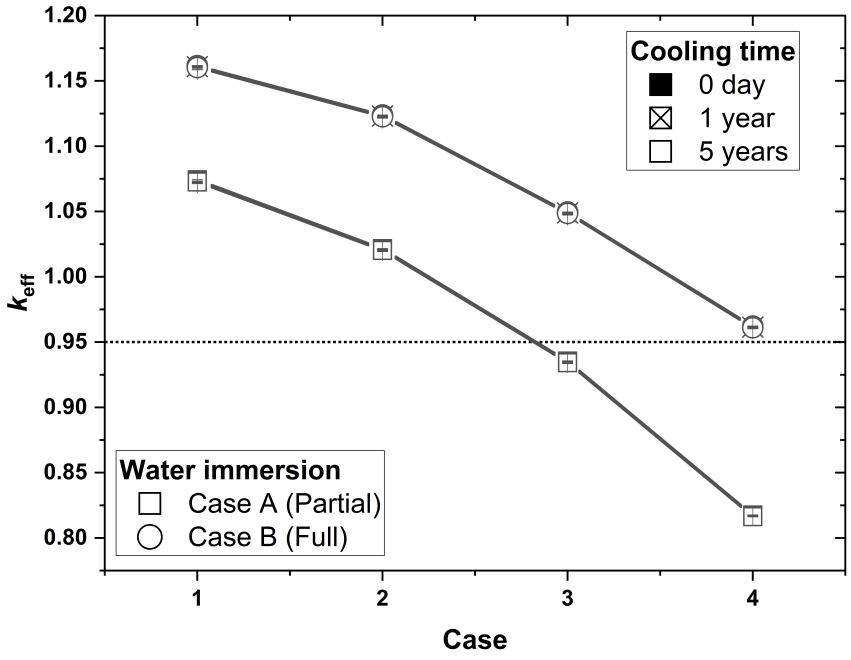

Figure 12. Multiplication factor of simulated criticality cases for irradiated fuel.

5. SCENARIO 3: SHIELDING ANALYSIS AND RADIATION DOSE DURING OPERATIONAL AND TRANSPORTATION OF SPENT FUEL

In this scenario, the shielding performance and radiation dose characteristics of the irradiated HPMR core were evaluated under two distinct conditions: during normal reactor operation and during postdischarge transportation. For a microreactor such as the HPMR, shielding during operation is just as critical as shielding during spent fuel transport. Unlike conventional large-scale reactors, microreactors are designed for deployment in remote locations with limited infrastructure. This design imposes strict constraints on the allowable size, weight, and material composition of shielding systems. The close proximity of the compact core to external surfaces, combined with high neutron and gamma fluxes, may present a challenge to maintaining radiation dose rates within regulatory and occupational safety limits. Moreover, the structural design of the HPMR, including heat pipe arrays and graphite monoliths, can introduce additional complexity because these components may become neutron activated over time and contribute to dose rates following reactor shutdown. Therefore, both operational and transport shielding scenarios were considered and evaluated.

5.1 DOSE RATE DURING OPERATION

The first shielding analysis evaluated the radiation dose environment surrounding the HPMR reactor enclosure under normal operating conditions. This assessment was performed near end of life, when the radiation from the core is expected to be most intense due to the buildup of fission products and actinides. The objective was to quantify neutron and photon dose rates external to the reactor structure and assess whether the assumed reactor enclosure and shielding design can maintain compliance with regulatory occupational dose limits.

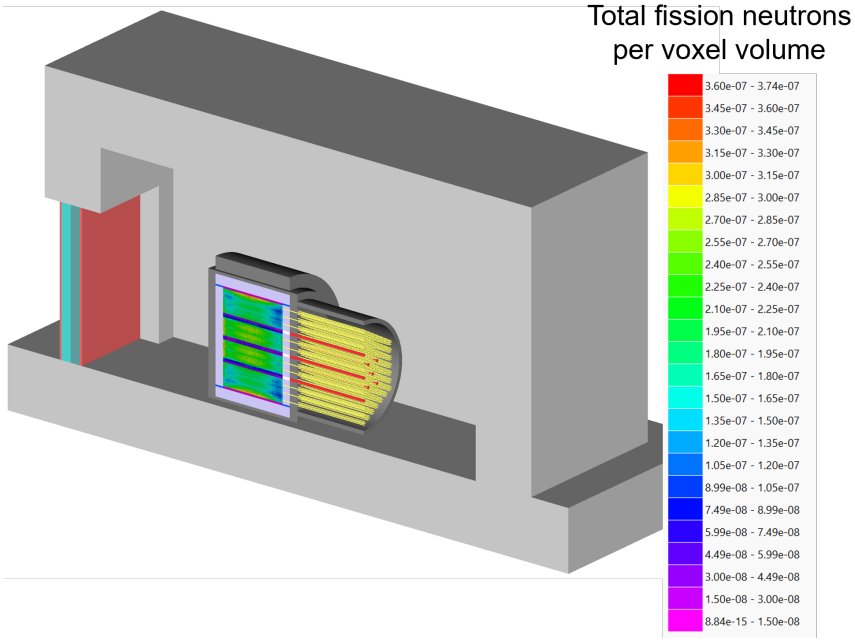

Figure 13. Fission source spatial distribution.

To characterize the source term for shielding analysis, a space- and energy-dependent prompt neutron fission source was generated using SCALE/TRITON-Shift. The core model was discretized into a $40 \times 40 \times 50$

spatial mesh with a 200-group neutron energy structure. The resulting volumetric fission source distribution, representing steady-state prompt neutron generation, was exported in HDF5 format and used as input for subsequent shielding calculations in SCALE/MAVRIC-Shift. As shown in Figure 13, the prompt neutron source is spatially confined to the fuel-containing regions of the core. The source distribution exhibits higher intensity near the periphery of the core due to localized spectral softening, particularly in areas adjacent to the BeO reflector. Prompt gamma radiation associated with the neutron fission source was also automatically generated within MAVRIC-Shift based on the prompt fission neutrons.

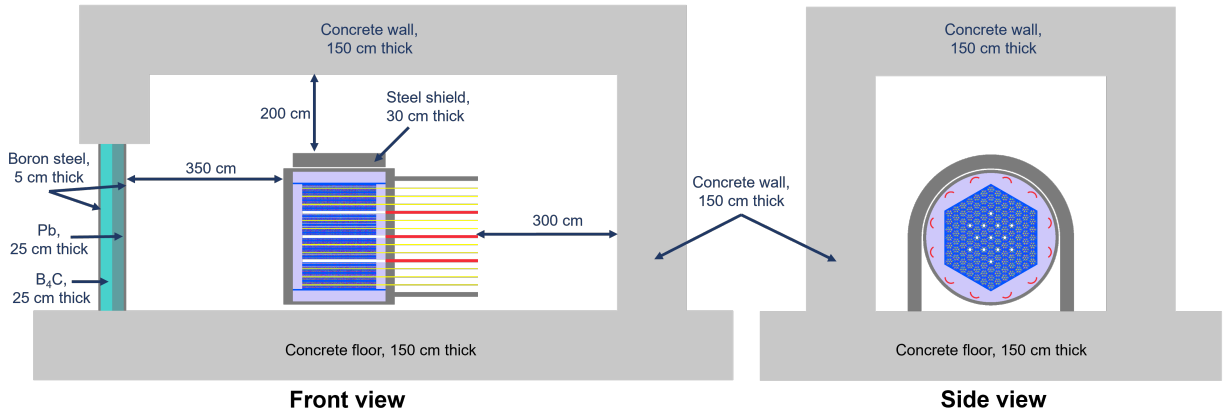

Figure 14. SCALE model for radiation shielding calculation of reactor enclosure.

The shielding model adopted for this analysis reflects a conservative, nonoptimized design. In the absence of publicly available reactor building specifications, a hypothetical geometry was assumed to illustrate general shielding behavior, as illustrated in Figure 14. The active core is enclosed within an inverted U-shaped stainless steel shield that is 30 cm thick, and additional 20 cm thick steel layers are placed above and below the core. The surrounding reactor enclosure is modeled as a 1.5 m thick concrete structure. A shielded access door composed of layered materials is also included; these materials include 5 cm of boron steel, 25 cm of lead, 25 cm of B_4C, and another 5 cm of boron steel. Only prompt neutron and gamma radiation were considered in this analysis. Although additional contributors such as delayed fission product decay and component activation can affect dose rates, their influence is expected to be minor during steady-state reactor operation and was therefore excluded for clarity and focus on dominant sources.

Figure 15 presents the calculated dose distributions around the reactor building. The total radiation dose rate at any point on the external surface of the enclosure remained below 0.5 rem/h. Specifically, the peak photon dose rate was approximately 0.3 rem/h, and the maximum neutron dose rate reached 0.5 rem/h. For reference, the annual occupational total effective dose equivalent is 5 rems (Code of Federal Regulations Title 10 Part 20). However, it should be noted that this configuration has not been optimized with respect to weight, cost, or deployability. Further refinement, such as advanced material selection, graded shielding, and optimized geometric arrangement, could further reduce external dose rates and tailor the system to meet specific requirements.

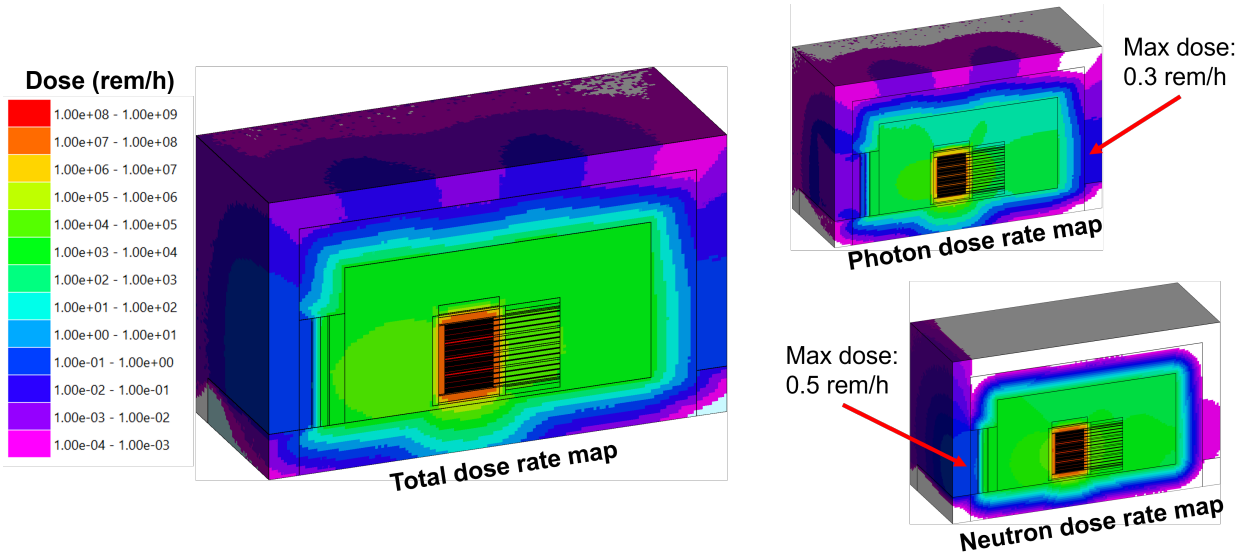

Figure 15. Operational dose rate distributions around the assumed HPMR reactor enclosure, showing total, photon, and neutron contributions.

5.2 DOSE RATE DURING TRANSPORTATION

This second shielding analysis evaluates radiation dose rates associated with the transportation of the irradiated HPMR core, including both unshielded and shielded conditions. The analysis consists of two parts: (1) an assessment of the unshielded dose rate to determine whether the core meets the physical protection threshold defined in 10 CFR 73 and (2) an evaluation of dose rates for a simplified transportation package under both normal and hypothetical accident conditions in accordance with 10 CFR 71 transport regulations.

Prior to the evaluation of shielding performance, an unshielded dose rate analysis was conducted to determine whether the irradiated core requires the physical protection measures specified in 10 CFR 73.37. According to this regulation, irradiated fuel must be protected by enhanced physical security if the unshielded dose rate exceeds 1 Gy/h (100 rad/h) at a distance of 1 m from any accessible surface (Code of Federal Regulations Title 10 Part 73). To evaluate this criterion, an unshielded MAVRIC-Shift model of the HPMR core was used to calculate the dose rate at 1 m for various postdischarge cooling times. The radiation source included contributions from fission product decay, actinide decay, and structural activation products; a 500 ppm cobalt impurity was assumed in stainless steel components.

For comparison, a typical high-burnup PWR fuel assembly with a discharge burnup of 50 GWd/tU was also evaluated using the same modeling approach. The results, shown in Figure 16, indicate that the unshielded HPMR core falls below the 100 rad/h threshold after approximately 7.7 years of cooling. It was also observed that activation products, particularly those arising from cobalt impurities in structural materials, contribute the dominant fraction of the total dose rate in the HPMR case. By contrast, the unshielded PWR fuel assembly remains above this threshold for more than 100 years. This difference is primarily attributable to the greater accumulation of long-lived actinides in the PWR fuel, including ^{244}Cm and ^{238}Pu, as a result of its higher burnup. These results indicate that the irradiated HPMR core requires enhanced physical protection during the first 7 to 8 years following discharge. After this period, the dose rate falls below the regulatory threshold, meaning that the physical protection requirements during storage and transportation are reduced.

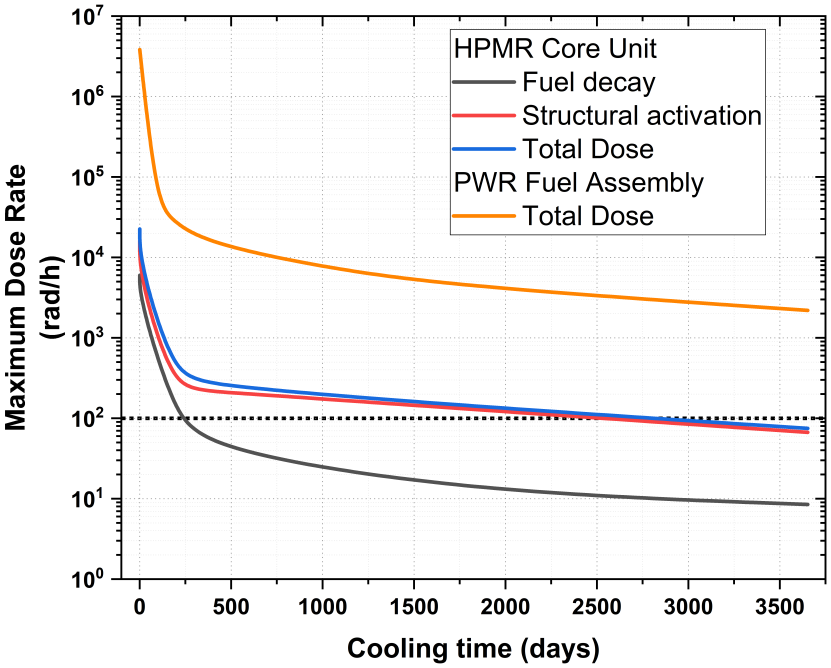

Figure 16. Comparison of maximum dose rate at 1 m for unshielded HPMR and PWR fuel as a function of cooling time.

Following the unshielded dose assessment, a second analysis was conducted to evaluate radiation dose rates during spent fuel transportation using a shielded configuration. It was assumed that the entire core would be transported as a single unit. A simplified cylindrical transport package was modeled. This model consisted of a 27 cm thick carbon steel shell for gamma attenuation and a 13 cm thick borated polyethylene resin layer for neutron shielding (Gauld and Ryman 2000). This configuration is intended to represent a generic package and has not been optimized for shielding performance, weight, or volume. The same postirradiation source terms used in the unshielded analysis were applied for consistency. Two transportation conditions were analyzed: the normal transport condition, in which the shielding package remains fully intact, and a hypothetical accident condition, in which the top section of the package is assumed to be breached, exposing part of the irradiated core to the external environment. The breached configuration is illustrated in Figure 17.

Figure 18 shows the dose rate distributions under both conditions. The numerical results are summarized in Table 6 and are compared directly against the regulatory limits defined in 10 CFR 71. Specifically, the allowable dose rate under normal transport conditions must not exceed 10 mrem/h at a distance of 2 m from the package surface. Under hypothetical accident conditions, the limit is 1 rem/h at 1 m from the external surface (Code of Federal Regulations Title 10 Part 71). The results indicate that under normal conditions, the dose rate remains well below the regulatory threshold at both 1 year and 5 year cooling periods. However, in the accident condition, the dose rate at 1 m exceeds the 1 rem/h limit at 1 year postdischarge, reaching approximately 1.21 rem/h. At 5 years of cooling, the dose rate falls to 0.67 rem/h, which is within regulatory bounds. These results demonstrate that although the current shielding design is sufficient to meet regulatory requirements under normal transportation conditions, compliance under accident scenarios is highly dependent on the postdischarge cooling time.

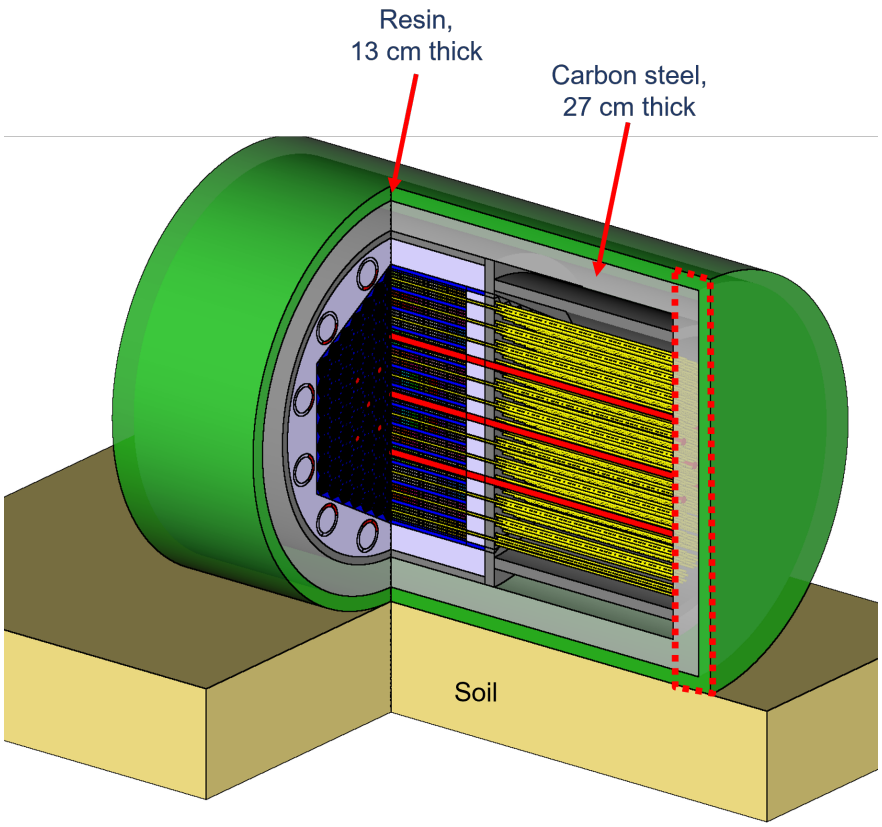

Figure 17. Assumed shielding configuration and accident breach condition (red outline) for transportation dose analysis.

Table 6. Calculated transportation dose rates compared with regulatory thresholds from 10 CFR 71

Cooling time	Condition	Dose rate	Regulatory limit
1 year	Normal (2 m)	0.05 mrem/h	10 mrem/h
	Accident (1 m)	1.21 rem/h	1 rem/h
5 years	Normal (2 m)	0.02 mrem/h	10 mrem/h
	Accident (1 m)	0.67 rem/h	1 rem/h

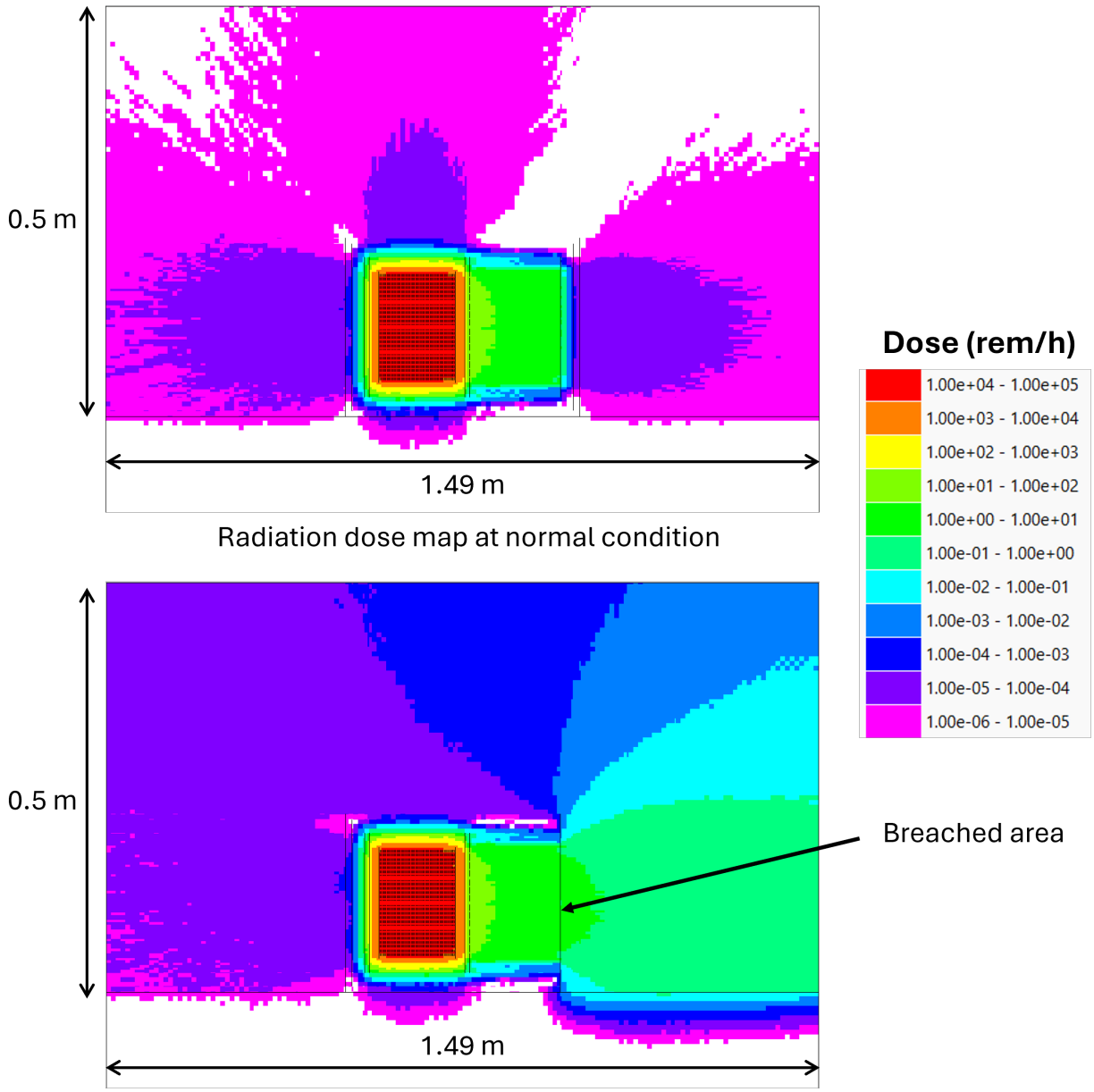

Figure 18. Dose rate distributions for normal (top) and hypothetical accident (bottom) transportation scenarios at 1 year of cooling.

6. CONCLUSIONS

This study demonstrates the application of SCALE version 6.3.2 and a development version of the 7.0 code system for evaluating nuclear criticality safety, radionuclide inventory, and radiation shielding across key stages of the nuclear fuel cycle for a TRISO-based HPMR. A generic HPMR design originally developed by Idaho National Laboratory was adapted and modified in this study as a representative microreactor concept featuring TRISO fuel compacts, heat pipe cooling, and a compact, transportable core layout. Three bounding scenarios were defined to evaluate SCALE's capabilities across normal operation, postirradiation transport, and relevant accident conditions without consideration of event probability.

In the first scenario, the criticality of the fresh core was evaluated under transportation-relevant accident conditions using SCALE's CSAS6 sequence with the Shift Monte Carlo neutron transport code. The analysis included bounding water immersion events, both partial and full, and considered multiple combinations of control rod and control drum positions. The results show that although partial immersion could be brought below the subcritical limit of $k_{\text{eff}} \leq 0.95$ using the existing control configuration, full immersion remained supercritical in all modeled cases, even with full insertion of control rods and inward-facing drum absorbers. Sensitivity studies on ^{10}B enrichment in the absorber materials demonstrated that increasing the absorber strength could reduce reactivity but is insufficient to meet subcriticality requirements alone. These findings suggest that supplemental design features, such as fixed neutron absorbers and enhanced control design, are necessary to satisfy the subcritical limit under this accident condition.

The second scenario extended the criticality assessment to the irradiated core. SCALE's TRITON depletion calculations, coupling Shift neutron transport calculations with the ORIGEN depletion and decay solver, were used to generate fuel inventories after 3 EFPY. Two control strategies were incorporated: (1) a conventional approach with fully withdrawn control drums and (2) a dynamic approach in which control drum angles were adjusted at each burnup step to maintain core criticality. The resulting postirradiation isotopic inventories were used to evaluate reactivity under partial and full immersion conditions. The irradiated core exhibited reduced reactivity due to fissile depletion and fission product accumulation. Under partial immersion, subcriticality was achieved with control rod insertion alone. However, full immersion still exceeded the k_{eff} limit, with the most favorable configuration reaching values up to 1,200 pcm above the subcritical threshold. Cooling time had minimal influence on reactivity; the difference between the 1 year and 5 year cases was less than 200 pcm. These findings again confirm that the current control system alone is not sufficient to ensure criticality under full immersion, even for irradiated fuel, and additional negative reactivity insertion, such as enhanced control design or burnable poisons, should be considered.

The third scenario focused on shielding and dose rate evaluations using SCALE's MAVRIC sequence in combination with Shift. During reactor operation, prompt neutron and gamma dose rates were calculated near the reactor enclosure boundary near end-of-life conditions. With assumptions for shielding geometry and materials, the total dose rate remained below 0.5 rem/h, dominated by the neutron component. This finding suggests that operational dose limits can be achieved using conventional shielding strategies and further optimized by considering cost and practicality. Transportation shielding was also analyzed using a simplified package consisting of carbon steel and resin. Under normal conditions, the package met all regulatory dose limits. However, under a hypothetical accident condition involving partial loss of shielding integrity, dose rates at 1 m exceeded the 1 rem/h threshold defined in 10 CFR 71 at 1 year of cooling. At 5 years of cooling, dose rates were within the regulatory limit, showing the importance of decay time in transport planning. Additionally, unshielded dose rate calculations were performed to assess physical protection requirements per 10 CFR 73. The HPMR core exceeded the 100 rad/h threshold for approximately 7.7 years, after which it no longer requires enhanced physical protection based on dose rate criteria. For

context, a typical PWR fuel assembly with 50 GWd/MTIHM burnup remains above this threshold for more than 100 years.

Overall, this study demonstrates the flexibility and integrated capabilities of the SCALE code system for analyzing compact microreactor systems across the nuclear fuel cycle. The coordinated use of CSAS6-Shift, TRITON-Shift, and MAVRIC-Shift enabled consistent modeling of TRISO-fueled core behavior from initial operation through spent fuel transport and storage. These analyses support the broader applicability of SCALE for non-LWR systems, including advanced, transportable reactor designs.

Several enhancements are planned for the SCALE code system to further support microreactor modeling and improve the user experience. These enhancements include enabling automatic and efficient placement of TRISO particles at high packing fractions (up to 61%, compared with the maximum of ~20% in SCALE 6.3.2 and the maximum of ~55% in the current development version of SCALE 7.0), parallelization of the cross section processing module to reduce the MG processing time for complex TRISO models, automated reactivity control search during depletion, adjoint-weighted kinetics parameter calculations, and memory reduction for CE and MG depletion calculations of models with randomly distributed TRISO particles.

7. REFERENCES

Borowski, J., M. Call, D. Dunn, A. Rigato, J. Smith, J. Solis, J. Tapp, and B. White. 2020. *Standard Review Plan for Transportation Packages for Spent Fuel and Radioactive Materia.* Technical report NUREG-2216. U.S. Nuclear Regulatory Commission. https://www.nrc.gov/docs/ML2023/ML20234A651.pdf.

Bostelmann, F., C. Celik, R. F. Kile, and W. A. Wieselquist. 2022. *SCALE Analysis of a Fluoride Salt-Cooled High-Temperature Reactor in Support of Severe Accident Analysis.* Technical report ORNL/TM-2021/2273. Oak Ridge, TN: Oak Ridge National Laboratory. https://doi.org/10.2172/1854475.

Bostelmann, F., C. Celik, M.L. Williams, R. J. Ellis, G. Ilas, and W. A. Wieselquist. 2020. "SCALE capabilities for high temperature gas-cooled reactor analysis." *Annals of Nuclear Energy* 147:107673. https://doi.org/10.1016/j.anucene.2020.107673.

Bostelmann, F., E. E. Davidson, W. A. Wieselquist, D. Luxat, K. C. Wagner, and L. I. Albright. 2023. *Non-LWR Fuel Cycle Scenarios for SCALE and MELCOR Modeling Capability Demonstration.* Technical report ORNL/TM-2023/2954. Oak Ridge, TN: Oak Ridge National Laboratory. https://doi.org/10.2172/2251628.

Bostelmann, F., S. E. Skutnik, A. Shaw, D. Hartanto, and W. A. Wieselquist. 2024. *SCALE 6.3 Modeling Strategies for Reactivity, Nuclide Inventory, and Decay Heat of Non-LWRs.* Technical report ORNL/TM-2024/3213. Oak Ridge, TN: Oak Ridge National Laboratory. https://doi.org/10.2172/2351061.

Chadwick, M.B., M. Herman, P. Obložinský, M.E. Dunn, Y. Danon, A.C. Kahler, D.L. Smith, et al. 2011. "ENDF/B-VII.1 Nuclear Data for Science and Technology: Cross Sections, Covariances, Fission Product Yields and Decay Data." *Nuclear Data Sheets* 112 (12): 2887–2996. https://doi.org/10.1016/j.nds.2011.11.002.

Code of Federal Regulations Title 10 Part 20. *Standards for Protection Against Radiation.* URL: https://www.ecfr.gov/current/title-10/part-20.

Code of Federal Regulations Title 10 Part 71. *Packaging and Transportation of Radioactive Material.* URL: https://www.ecfr.gov/current/title-10/chapter-I/part-71.

Code of Federal Regulations Title 10 Part 73. *Physical Protection of Plants and Materials.* URL: https://www.ecfr.gov/current/title-10/chapter-I/part-73.

De Hart, M. D., and S. M. Bowman. 2011. "Reactor Physics Methods and Analysis Capabilities in SCALE." *Nuclear Technology* 174 (2): 196–213. https://doi.org/10.13182/NT174-196.

Elzohery, R., D. Hartanto, F. Bostelmann, and W. A. Wieselquist. 2024. *SCALE Analyses of Scenarios in the High-Temperature Gas-Cooled Reactor Fuel Cycle.* Technical report ORNL/TM-2024/3536. Oak Ridge, TN: Oak Ridge National Laboratory.

Evans, T. M., A. S. Stafford, R. N. Slaybaugh, and K. T. Clarno. 2010. "Denovo: A New Three-Dimensional Parallel Discrete Ordinates Code in SCALE." *Nuclear Technology* 171 (2): 171–200. https://doi.org/10.13182/NT171-171.

G. Radulescu, F. Bostelmann, D. Hartanto, and W. A. Wieselquist. 2025. "SCALE Shielding Calculations for Advanced Reactor Accident Scenarios." *Nuclear Science and Engineering,* https://doi.org/10.1080/00295639.2025.2503125.

Gauld, I. C., and J. C. Ryman. 2000. *Nuclide Importance to Criticality Safety, Decay Heating, and Source Terms Related to Transport and Interim Storage of High-Burnup LWR Fuel.* Technical report NUREG/CR-6700; ORNL/TM-2000/284. Oak Ridge, TN: Oak Ridge National Laboratory. https://doi.org/10.2172/799527. https://www.nrc.gov/docs/ML0103/ML010330186.pdf.

Ghaddar, Tarek, Friederike Bostelmann, Tara Pandya, and Matthew Jessee. 2024. "Modeling Enhancements and Benchmarking of Pebble Bed Reactors in the Shift Monte Carlo Code." In *International Conference on Physics of Reactors (PHYSOR 2024).* https://www.osti.gov/biblio/2397462.

Goluoglu, S., L. M. Petrie Jr, M. E. Dunn, D. F. Hollenbach, and B. T. Rearden. 2011. "Monte Carlo criticality methods and analysis capabilities in SCALE." *Nuclear Technology* 174 (2): 214–235. https://doi.org/10.13182/NT10-124.

Hartanto, D., G. Radulescu, F. Bostelmann, and W. Wieselquist. 2025. *SCALE Analyses of Scenarios in the Molten Salt Reactor Fuel Cycle.* Technical report ORNL/TM-2024/3659. Oak Ridge, TN: Oak Ridge National Laboratory.

Hartanto, D., G. Radulescu, F. Bostelmann, and W. A. Wieselquist. 2024. *SCALE Demonstration for Sodium-Cooled Fast Reactor Fuel Cycle Analysis.* Technical report ORNL/TM-2023/3214. Oak Ridge, TN: Oak Ridge National Laboratory. https://doi.org/10.2172/2341402.

Humphries, L. L., B. A. Beeny, F. Gelbard, D. L. Louie, J. Phillips, R. C. Schmidt, and N. E. Bixler. 2021. *MELCOR Computer Code Manuals - Vol. 1: Primer and Users' Guide Version 2.2.18019.* Technical report SAND2021-0726 O. Albuquerque, NM: Sandia National Laboratories. https://www.nrc.gov/docs/ML2104/ML21042B319.pdf.

Kim, Kang Seog, Andrew M. Holcomb, F. Bostelmann, Dorothea Wiarda, Brandon R Langley, and William Wieselquist. 2021. "Improvement of the SCALE-XSProc Capability for High-Temperature Gas-Cooled Reactor Analysis." In *International Conference on Mathematics and Computational Methods Applied to Nuclear Science and Engineering (M&C 2021).* https://www.osti.gov/biblio/1826043.

Lo, A., F. Bostelmann, D. Hartanto, B. Betzler, and W. A. Wieselquist. 2022. *Application of SCALE to Molten Salt Fueled Reactor Physics in Support of Severe Accident Analyses.* Technical report ORNL/TM-2022/1844. Oak Ridge, TN: Oak Ridge National Laboratory. https://doi.org/10.2172/1897864.

Ortensi, J., M. K. Jaradat, J. E. Hansel, and S. Terlizzi. 2024. *The Monolithic Heat Pipe Microreactor Reference Plant Model.* Technical report INL/RPT-24-77914. Idaho Falls, ID: Idaho National Laboratory. https://doi.org/10.2172/2356755.

Pandya, T. M., S. R. Johnson, T. M. Evans, G. G. Davidson, S. P. Hamilton, and A. T. Godfrey. 2016. "Implementation, Capabilities, and Benchmarking of Shift, a Massively Parallel Monte Carlo Radiation Transport Code." *Journal of Computational Physics* 308:239–272. https://doi.org/10.1016/j.jcp.2015.12.037.

Peplow, D. E. 2011. "Monte Carlo Shielding Analysis Capabilities with MAVRIC." *Nuclear Technology* 174 (2): 289–313. https://doi.org/10.13182/NT174-289.

Shaw, A., F. Bostelmann, D. Hartanto, E. Walker, and W. A. Wieselquist. 2023. *SCALE Modeling of the Sodium-Cooled Fast-Spectrum Advanced Burner Test Reactor.* Technical report ORNL/TM-2022/2758. Oak Ridge, TN: Oak Ridge National Laboratory. https://doi.org/10.2172/1991734.

Skutnik, S. E., and W. A. Wieselquist. 2021. *Assessment of ORIGEN Reactor Library Development for Pebble-Bed Reactors Based on the PBMR-400 Benchmark.* Technical report ORNL/TM-2020/1886. Oak Ridge, TN: Oak Ridge National Laboratory. https://doi.org/10.2172/1807271.

Sowder, A., and C. Marciulescu. 2020. *Uranium Oxycarbide (UCO) Tristructural Isotropic (TRISO)-Coated Particle Fuel Performance.* Technical report Topical Report EPRI-AR-1(NP)-A. Palo Alto, CA: Electric Power Research Institute. https://www.epri.com/research/products/000000003002019978.

US NRC. 2020. *NRC Non-Light Water Reactor (Non-LWR) Vision and Strategy, Volume 3: Computer Code Development Plans for Severe Accident Progression, Source Term, and Consequence Analysis.* Technical report ML20030A178, Rev. 1. Rockville, MD: US Nuclear Regulatory Commission. https://www.nrc.gov/docs/ML2003/ML20030A178.pdf.

———. 2021. *NRC Non-Light Water Reactor (Non-LWR) Vision and Strategy, Volume 5: Radionuclide Characterization, Criticality, Shielding, and Transport in the Nuclear Fuel Cycle.* Technical report ML21088A047, Rev. 1. Rockville, MD: US Nuclear Regulatory Commission. https://www.nrc.gov/docs/ML2108/ML21088A047.pdf.

Wagner, K., B. Beeny, T. Haskin, D. Luxat, and R. Schmidt. 2023. *MELCOR Accident Progression and Source Term Demonstration Calculations for a Molten Salt Reactor.* Technical report SAND2023-01803. Albuquerque, NM: Sandia National Laboratories. https://www.nrc.gov/docs/ML2311/ML23117A094.pdf.

Wagner, K., B. Beeny, and D. Luxat. 2022. *MELCOR Accident Progression and Source Term Demonstration Calculations for a HTGR.* Technical report SAND2022-2750. Albuquerque, NM: Sandia National Laboratories. https://www.osti.gov/biblio/1854083.

———. 2023. *MELCOR Accident Progression and Source Term Demonstration Calculations for a Sodium Fast Reactor (SFR).* Technical report SAND2023-10830. Albuquerque, NM: Sandia National Laboratories. https://www.nrc.gov/docs/ML2328/ML23285A093.pdf.

Wagner, K., C. Faucett, R. Schmidt, and D. Luxat. 2022. *MELCOR Accident Progression and Source Term Demonstration Calculations for a Heat Pipe Reactor.* Technical report SAND2022-2745. Albuquerque, NM: Sandia National Laboratories. https://www.osti.gov/biblio/1854082.

Wagner, K., T. Haskin, B. Beeny, F. Gelbard, and D. Luxat. 2022. *MELCOR Accident Progression and Source Term Demonstration Calculations for a FHR.* Technical report SAND2022-2751. Albuquerque, NM: Sandia National Laboratories. https://www.osti.gov/biblio/1854081.

Walker, E., S. E. Skutnik, W. A. Wieselquist, A. Shaw, and F. Bostelmann. 2021. *SCALE Modeling of the Fast-Spectrum Heat Pipe Reactor.* Technical report ORNL/TM-2021/2021. Oak Ridge, TN: Oak Ridge National Laboratory. https://doi.org/10.2172/1871124.

Wieselquist, W., and R. A. Lefebvre. 2023. *SCALE 6.3.1 User Manual.* Technical report ORNL/TM-SCALE-6.3.1. Oak Ridge, TN: Oak Ridge National Laboratory. https://doi.org/10.2172/1959594.